

UVA/persulfate-driven nonylphenol polyethoxylate degradation: effect of process conditions

R. F. Nunes, F. K. Tominaga, S. I. Borrely & A. C. S. C. Teixeira

To cite this article: R. F. Nunes, F. K. Tominaga, S. I. Borrely & A. C. S. C. Teixeira (2022) UVA/persulfate-driven nonylphenol polyethoxylate degradation: effect of process conditions, Environmental Technology, 43:2, 286-300, DOI: [10.1080/09593330.2020.1786166](https://doi.org/10.1080/09593330.2020.1786166)

To link to this article: <https://doi.org/10.1080/09593330.2020.1786166>

 View supplementary material [↗](#)

 Published online: 04 Jul 2020.

 Submit your article to this journal [↗](#)

 Article views: 169

 View related articles [↗](#)

 View Crossmark data [↗](#)

 Citing articles: 3 View citing articles [↗](#)



UVA/persulfate-driven nonylphenol polyethoxylate degradation: effect of process conditions

R. F. Nunes ^a, F. K. Tominaga ^b, S. I. Borrely ^b and A. C. S. C. Teixeira ^a

^aResearch Group in Advanced Oxidation Processes (AdOx), Department of Chemical Engineering, Escola Politécnica, University of São Paulo, São Paulo, Brazil; ^bLaboratory of Biological and Environmental Assays, Radiation Technology Center, Energy and Nuclear Research Institute, São Paulo, Brazil

ABSTRACT

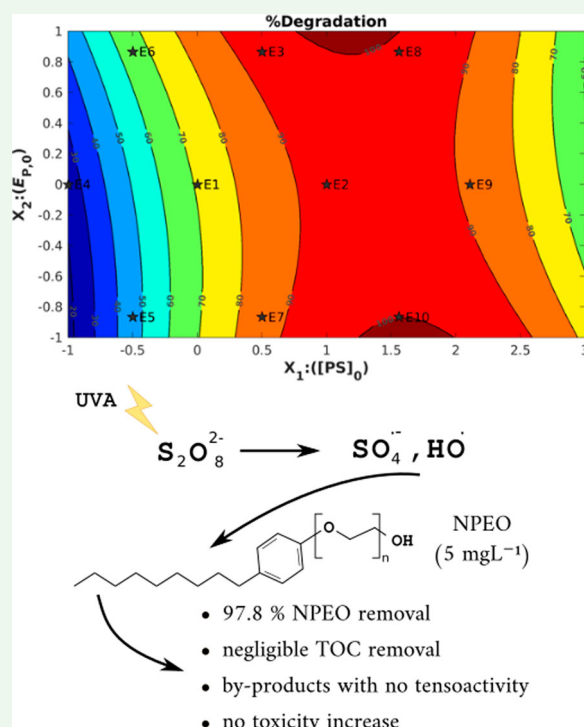
UV/persulfate (UV/PS) technologies have gained increased attention as efficient alternatives for removing pollutants from different classes, although processes based on the UVA-driven $S_2O_8^{2-}$ (PS) activation have not yet been discussed in the literature for the removal of the nonionic surfactant nonylphenol polyethoxylate (NPEO). The present study investigated the simultaneous effect of the initial persulfate concentration ($[PS]_0$) and specific photon emission rate ($E_{p,0}$) on NPEO degradation by UVA/PS following a Doehlert experimental design. The results for $[NPEO]_0 = (4.65 \pm 0.15) \text{ mg L}^{-1}$ indicated more than 97.8% NPEO removal after 2 h, with pseudo first-order specific degradation rate (k_{obs}) of 0.0320 min^{-1} , for $[PS]_0 = 7.75 \text{ mmol L}^{-1}$ and $E_{p,0} = 0.437 \text{ } \mu\text{mol photons L}^{-1} \text{ s}^{-1}$. Under these conditions, NPEO half-life time was about 22 min, and the $EC_{50-48 \text{ h}}$ (% v/v) values for *Daphnia similis* before and after treatment did not differ significantly. Higher values of $E_{p,0}$ would influence NPEO removal for $[PS]_0$ not higher than 8–10 mmol L^{-1} , although lower degradation efficiencies were obtained with higher $[NPEO]_0$ or real wastewater, except for longer reaction times. Additionally, UVA/PS showed to be efficient for tensoactivity removal, despite the negligible total organic carbon (TOC) removal achieved. Finally, UVC and UVA resulted in NPEO degradation higher than 96% and similar tensoactivity removals when UVA/PS was conducted under optimal conditions ($[PS]_0 = 10 \text{ mmol L}^{-1}$; $E_{p,0} = 0.324 \text{ } \mu\text{mol photons L}^{-1} \text{ s}^{-1}$), suggesting that UVA radiation available in solar light could be advantageously employed for NPEO removal at concentrations usually found in wastewater.

ARTICLE HISTORY

Received 13 January 2020
Accepted 16 June 2020

KEYWORDS

Surfactants; nonylphenol polyethoxylate; persulfate; UVA; surface tension



CONTACT R. F. Nunes  robertafrinhani@usp.br  Research Group in Advanced Oxidation Processes (AdOx), Department of Chemical Engineering, Escola Politécnica, University of São Paulo, Av. Prof. Luciano Gualberto, tr. 3, 380, São Paulo, Brazil

 Supplemental data for this article can be accessed at <https://doi.org/10.1080/09593330.2020.1786166>

© 2020 Informa UK Limited, trading as Taylor & Francis Group

Introduction

Contaminants of emerging concern (CECs) have been arising as a challenge due to their persistence and continuous introduction into aquatic environments. CECs include pharmaceuticals and personal care products (PCPs), plasticisers, food additives, wood preservatives, laundry detergents, surfactants, disinfectants, flame retardants, pesticides, natural and synthetic hormones, disinfection by-products, among others [1]. Surfactant molecules contain at least one hydrophobic and one hydrophilic moiety and are classified as anionic, cationic, amphoteric and nonionic, according to the charge of the head group [2]. Among them, nonionic nonylphenol polyethoxylate (NPEO) is used in diverse applications, such as laundering, textile processing, pulp and paper processing, paint and resin formulation, oil and gas recovery, steel manufacturing, pest control, power generation, personal care products, cleaners and detergents, among others [3,4].

As a consequence of the widespread use and high consumption, NPEO occurs persistently in the environment, and can be released into aquatic systems predominantly via municipal and industrial wastewater discharges [3]. According to the literature, these compounds have been detected in textile industry wastewater in concentrations up to $0.93\text{--}5.68\text{ mg L}^{-1}$ [5]. In sewage effluents and treated sludge, alkylphenol ethoxylates have been reported in concentrations of up to 0.33 mg L^{-1} and 81 mg kg^{-1} , respectively [6], and in wastewaters from six commercial laundries, NPEO has been found at concentrations ranging between 1.6 mg L^{-1} and 108.937 mg L^{-1} [7]. High concentrations ($0.075\text{--}4.12\text{ mg L}^{-1}$) of NP9EO were also found in a hospital wastewater treatment plant (WWTP) [8]. The occurrence of NPEO in different water matrices reinforces the importance of finding efficient technologies for treating wastewater containing this emerging class of contaminants.

Three technologies are used for treating wastewaters contaminated by surfactants: (i) physical methods employing precipitation, adsorption, flocculation, electro-flocculation, and others; (ii) chemical methods including advanced oxidation and reduction processes; and (iii) biological methods based on aerobic and anaerobic degradation [9]. Regarding biodegradation, previous studies indicate that this process can originate by-products more toxic than the parent-compounds (e.g. nonylphenol), with bioaccumulative and endocrine disruptive characteristics [4,10–15]. Alternatively, advanced oxidation processes (AOPs), such as ultraviolet radiation combined with the persulfate anion ($\text{S}_2\text{O}_8^{2-}$) (UV/PS), have gained increased attention as efficient

alternatives for removing pollutants from different classes, generating sulfate radicals *in situ* with a high standard reduction potential ($2.5\text{--}3.1\text{ V SHE}$) when compared to other radical species such as HO^\bullet (2.8 V SHE) [16]. PS also presents the advantage of being activated by longer wavelengths, such as UVA radiation. In fact, the molar absorption coefficients of hydrogen peroxide and persulfate (peroxydisulfate, PS) at 254 nm are close, i.e. $18.6\text{ L mol}^{-1}\text{ cm}^{-1}$ and $13.8\text{--}14.0\text{ L mol}^{-1}\text{ cm}^{-1}$, respectively [17]; comparatively, the molar absorption coefficient of ozone at this same wavelength is much higher, of about $2760 \pm 200\text{ L mol}^{-1}\text{ cm}^{-1}$ [18]. In contrast, when the UVA region is considered, persulfate has a higher molar absorption coefficient in comparison with H_2O_2 , with values of $0.25\text{ L mol}^{-1}\text{ cm}^{-1}$ at 351 nm for persulfate [19] and only $0.01\text{ L mol}^{-1}\text{ cm}^{-1}$ at 360 nm for H_2O_2 [20]; the value of ϵ for PS is of the same order of magnitude as that of O_3 ($\epsilon = 0.61\text{ L mol}^{-1}\text{ cm}^{-1}$ at 350 nm) [21]. In addition, PS salts are stable solids at room temperature [22] and can be easily transported and stored, which are quite advantageous characteristics in comparison with other traditional oxidants.

In previous studies, the efficient removal of surfactants by means of biochar-supported zero valent iron composite/persulfate [23], electro/ Fe^{2+} /persulfate [24], and UVC/ $\text{K}_2\text{S}_2\text{O}_8$ [25–28] was achieved for nonionic surfactants (e.g. 4-nonylphenol; Triton X-45/octylphenol polyethoxylate; Brij30/polyoxyethylated lauryl ether), and for an anionic surfactant (SDBS/sodium dodecylbenzene sulfonate). The literature reports a few studies devoted to CECs removal by the UVA/PS process. According to Wang and Wang [29], 3-chlorophenol and 4-chlorophenol were completely degraded after 1.5 h by the UVA/PS process under the following conditions: initial pollutant concentration of 0.2 mmol L^{-1} , initial PS concentration of 10 mmol L^{-1} , and pH 4. Palharim et al. [30] obtained 77.3% propylparaben removal using 7.25 mmol L^{-1} PS concentration, while total degradation of the pesticide amicarbazone was achieved for PS concentration of 5 mmol L^{-1} , initial pollutant concentration of $41.4\text{ }\mu\text{mol L}^{-1}$ and pH 7 [31]. Additionally, Ioannidi, Frontistis and Mantzavinos [22] found that UV-A radiation from LEDs or solar light to activate persulfate can readily degrade parabens at concentrations found in the environment.

In order to contribute to the knowledge on the use of PS-driven processes in wastewaters treatment, the present study investigates the UVA-activated PS process for the degradation of NPEO containing nine ethoxylate groups (NP9EO). The simultaneous effects of the initial persulfate concentration ($[\text{PS}]_0$) and specific

photon emission rate ($E_{p,0}$) on surfactant degradation and tensoactivity removal were investigated and optimised following a Doehlert experimental design. Then, the optimum conditions were fixed, and the influence of other important parameters for the practical application of the process under study, such as initial NPEO concentration, radiation wavelength and water matrix, were explored. The toxicity of the treated solution obtained after applying the best operational conditions was analysed against *Daphnia similis*. As far as we are concerned, all these aspects have not been simultaneously discussed in the literature.

Materials and methods

Chemicals

Technical grade (95%) and analytical grade samples of NPEO ($C_9H_{19}C_6H_4(OCH_2CH_2)_nOH$, CAS 9016-45-9) were obtained from Oxiteno and Sigma-Aldrich, respectively, and used with no further purification. Sodium persulfate was obtained from Merck ($\geq 99\%$). HPLC-grade acetonitrile and methanol were obtained from Sigma-Aldrich ($\geq 99.9\%$). Aqueous solutions were prepared using Milli-Q® water, obtained from a Milli-Q® Direct-Q system (Merck Millipore) (18.2 MΩ cm), except when the influence of a real water matrix was investigated. For this purpose, a sample collected from a WWTP and decanted before characterisation (Table S1), was used instead.

Photo-oxidation experiments

Photodegradation experiments were carried out in a magnetically-stirred quartz beaker (Figure S1), containing 250 mL NP9EO solution irradiated by two, three or four 15-W backlight lamps (Sylvania F15W/350 BL T8) emitting 5.3, 7.8 and 10.5 W m⁻² UVA radiation ($\lambda_{max} = 354$ nm, Figure S2(a)), respectively. The lamps were positioned over the beaker, at 20 cm from the liquid surface. UVC-driven experiments were carried out in the same experimental apparatus, using one or two 8-W lamps (Philips TUV 8W/G8T5) positioned at 14.5 cm from the liquid surface, emitting 4.8 and 11.4-W m⁻² ($\lambda_{max} = 254$ nm, Figure S2(b)), respectively. The irradiance of both radiation sources was determined for each system by means of a spectroradiometer (Luzchem, SPR-4002). Measured spectral irradiances (mW m⁻² nm⁻¹) were converted to (mol photons m⁻² s⁻¹ nm⁻¹) using the Planck equation. These values were further integrated in the wavelength ranges 300–400 nm (UVA) or 250–260 nm (UVC), and then multiplied by the surface area of the liquid contained in the beaker, and divided by its volume in order to obtain $E_{p,0}$ in (μmol photons L⁻¹ s⁻¹).

The working initial NPEO concentrations used herein (1–24 mg L⁻¹) were selected within the range of values found in the literature for real water matrices, as aforementioned. This concentration range is below the CMC (critical micelle concentration) of 34 mg L⁻¹ for NPEO containing an average of 9.5 ethoxy units [32]. The necessary mass of solid sodium persulfate was added to the NPEO-containing solution just before the irradiation was turned on, to achieve the desired PS concentration. In all the experiments, the liquid temperature was kept at (20 ± 2) °C using a circulating water bath; the initial pH was 4.2 ± 0.2, and not corrected over the irradiation time. At each sampling time, 1 mL was collected from the reaction medium and mixed with MeOH (10% final concentration) to stop the reaction, following the procedure used by Graça et al. [31]. Control experiments were performed in the absence of either UVA or PS.

Doehlert design for two variables and response surface model

A Doehlert design [33] (Table 1 and Figure S3) was chosen to find the best conditions for NPEO removal by the UVA/PS process; the response variables were the NPEO percent degradation after 120 min of irradiation and the pseudo first-order specific degradation rate. The characteristics and advantages of this design are fully described by Ferreira et al. [34]. The number of experiments is given by $n^2 + n + cp$, where n is the number of factors evaluated, and cp corresponds to the number of replicates of the central point [35]. The initial PS concentration (codified variable X_1) was varied at seven levels (1; 3.25; 5.5; 10;

Table 1. Original Doehlert design (Exps. 1–7) and additional runs (Exps. 8–10) for NPEO degradation by the UVA/PS process. $[NPEO]_0 = (4.65 \pm 0.15)$ mg L⁻¹

Exp.	X_1 : $[PS]_0$ (mmol L ⁻¹)		X_2 : Number of lamps/ $E_{p,0}$ (μmol photons L ⁻¹ s ⁻¹)		Response variables (120 min)	
	Coded values	Real values	Coded values	Real values	% Degradation	k_{obs}
1	0	5.5	0	3 / 0.324	69.3*	0.0093**
2	1	10	0	3 / 0.324	96.1	0.0237
3	0.5	7.75	0.866	4 / 0.437	97.8	0.0320
4	-1	1	0	3 / 0.324	21.6	0.0020
5	-0.5	3.25	-0.866	2 / 0.212	49.6	0.0059
6	-0.5	3.25	0.866	4 / 0.437	66.7	0.0083
7	0.5	7.75	-0.866	2 / 0.212	85.9	0.0144
8	1.56	12.5	0.866	4 / 0.437	93.2	0.0671
9	2.11	15	0	3 / 0.324	93.1	0.050
10	1.56	12.5	-0.866	2 / 0.212	96.0	0.0272

*Performed in triplicate, giving (69.3 ± 1.3) %; **Performed in triplicate, giving (0.0093 ± 0.0008) min⁻¹; k_{obs} : pseudo first-order specific degradation rate, with R^2 in the range 0.93–0.99.

7.75, 12.5 and 15 mmol L⁻¹); the aim consisted in identifying the values of PS concentration which would significantly promote surfactant degradation, and also the threshold concentration values from which PS would act as a scavenger. The number of lamps (codified variable X_2) was evaluated at three levels (2, 3 and 4) fitting the dimensions of the reaction cabinet used (Figure S1), such that the system would not be over irradiated; the corresponding $E_{p,0}$ values were 0.212, 0.324, and 0.437 $\mu\text{mol photons L}^{-1} \text{s}^{-1}$, respectively. Experiment E1 was performed in triplicate to assess the experimental error.

Polynomial regression models were fitted to experimental results using the least squares method with the aid of Statgraphics® and Matlab software. The response surface model is a second-order polynomial equation (Eq. 1), where y is the response variable and X_1 and X_2 correspond to the independent variables:

$$y = a + bX_1 + cX_2 + dX_1^2 + eX_2^2 + fX_1X_2 \quad (1)$$

Additional experiments were performed to evaluate the influence of the initial NPEO concentration, the effect of a lower wavelength on persulfate activation, and the effect of the constituents of a real wastewater on the performance of the UV/PS process for removing NPEO. The experimental conditions in each case are detailed in the corresponding sections.

Analytical methods

NPEO concentration was determined by high performance liquid chromatography (Shimadzu, LC20 model), using a RP18 column (250 mm \times 4.6 mm; 5 μm) and a UV-vis detector (Shimadzu, SPD20A model). The isocratic elution consisted of 70% acetonitrile and 30% water at a flow rate of 1.2 mL min⁻¹. The injection volume was 50 μL and the detection wavelength was 226 nm. Under these conditions, NPEO retention time was 12 min. The detection and quantification limits were 0.0676 and 0.2028 mg L⁻¹, respectively.

Total organic carbon (TOC) analyses were carried out in a TOC-L analyzer (Shimadzu).

Surface tension was measured using the Du Noüy ring method, using a tensiometer (Model K6 96602, KRÜSS GmbH Germany). Surface tension reductions relative to Milli-Q® water ($\Delta\gamma_{\text{rel}}$) were calculated by Eq. 2, in which $\gamma_{\text{H}_2\text{O}}$ and γ_{sample} refer to the surface tensions of Milli-Q® water and sample, respectively:

$$\Delta\gamma_{\text{rel}} = \left(\frac{\gamma_{\text{H}_2\text{O}} - \gamma_{\text{sample}}}{\gamma_{\text{H}_2\text{O}}} \right) \times 100 \quad (2)$$

Ecotoxicity assays

Acute ecotoxicity assays with the microcrustacean *Daphnia similis* were performed before and after the UVA/PS treatment using the condition of the highest NPEO removal achieved by the Doehlert experimental design. The assays were conducted at the Laboratory of Biological and Environmental Assays (Nuclear and Energy Research Institute-IPEN-CNEN/SP, São Paulo, Brazil), according to the methodology described in the Brazilian Standard ABNT NBR 12713/2016 [36].

Serial dilutions (100%, 75%, 50%, 25%, 12.5%) of the solutions to be analyzed were prepared using culture water (see Supplementary Information, Section S1, for further details), existing 4 replicates for each dilution; the culture water was used as the control solution, also in 4 replicates. Each one of these solutions was inoculated with 5 neonates of *D. similis* with 6–24 h of life. Organisms were exposed to the samples for 48 h at (20 \pm 1) °C. Physicochemical parameters (pH, dissolved oxygen and conductivity) were controlled before and after ecotoxicity assays.

At the end of 48 h, the number of immobile organisms in each sample was counted. The effect concentrations that promoted 50% immobility of exposed living organisms ($\text{EC}_{50-48 \text{ h}}$, expressed in % v/v), and the respective confidence intervals were obtained with the aid of the Trimmed Spearman-Kärber statistical test [37].

Results and discussion

Control experiments indicate that neither PS alone (in the dark) nor direct UVA/UVC photolysis promote significant NPEO degradation. In fact, NPEO absorbs mainly at 224 and 275 nm in aqueous solution, with no absorption observed at wavelengths higher than 300 nm, as reported in previous studies [38,39]. It is worth observing that the UVC lamp used does not emit at 275 nm (Figure S2(b)), while the UVA lamp exhibits a slight emission at this wavelength (Figure S2(a)), which was not sufficient for NPEO direct photolysis, that can only take place at wavelengths where photolysis quantum yields are sufficiently high.

In order to evaluate the simultaneous effect of the specific photon emission rate ($E_{p,0}$) and initial persulfate concentration $[\text{PS}]_0$ on NPEO degradation by UVA/PS, twelve experiments were performed following the Doehlert design; the time-variation of NPEO concentration for each run is shown in Figure 1. The main results are summarised in Table 1, showing that NPEO removals and k_{obs} varied in the ranges 21.6–97.8% and 0.0020–0.0671 min⁻¹, respectively. Moreover, the time evolution of $[\text{NPEO}]$ depended strongly on the combination of $[\text{PS}]_0$

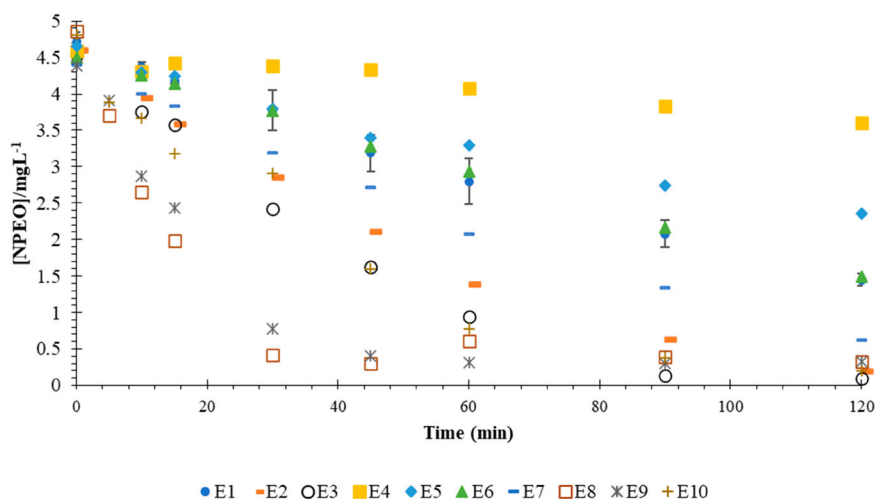


Figure 1. Time-variation of NPEO concentration for each run of the Doehlert design. Conditions: $[\text{NPEO}]_0 = (4.65 \pm 0.15) \text{ mg L}^{-1}$; $\text{pH}_0 = 4.2 \pm 0.2$; temperature = $(20 \pm 2) \text{ }^\circ\text{C}$.

and $E_{p,0}$ (Figure 1). For example, a slight decrease in NPEO concentration after 120 min was observed in Exp. E4, carried out with $[\text{PS}]_0 = 1 \text{ mmol L}^{-1}$ and $E_{p,0} = 0.324 \text{ } \mu\text{mol photons L}^{-1} \text{ s}^{-1}$, resulting in the lowest values of NPEO percent degradation and k_{obs} . In contrast, NPEO concentration decreased fast in the first 45 min of irradiation in Exps. E8 and E9, for which $[\text{PS}]_0$ was 12.5 and 15 mmol L^{-1} , respectively, and $E_{p,0}$ was set at 0.437 and 0.324 $\text{ } \mu\text{mol photons L}^{-1} \text{ s}^{-1}$, respectively; in fact, for these runs, the values of k_{obs} were equal to 0.0671 and 0.050 min^{-1} , respectively, both achieving about 93% NPEO degradation after 120 min of irradiation. Nevertheless, the highest NPEO percent removal (97.8%) was achieved in Exp. E3, performed with a lower initial persulfate concentration (7.75 mmol L^{-1}) and $E_{p,0} = 0.437 \text{ } \mu\text{mol photons L}^{-1} \text{ s}^{-1}$, although in this case the surfactant concentration decreased more slowly with time ($k_{\text{obs}} = 0.0320 \text{ min}^{-1}$). In summary, a closer look at the results depicted in Figure 1 reveals that in some cases increasing $E_{p,0}$ can counterbalance lower initial persulfate concentrations, and vice versa, resulting in close NPEO concentration-time curves.

Effect of specific photon emission rate and initial persulfate concentration

Regarding the NPEO percent degradation after 120 min, the ANOVA obtained considering the original experimental design (Exps. E1-E7, plus the two replicates of Exp. E1) indicated that the effects $[\text{PS}]_0$, $[\text{PS}]_0^2$, $E_{p,0}$ and $(E_{p,0})^2$ were statistically significant (F test with p -value < 0.05), as shown by the Pareto chart; the determination coefficient of the corresponding response surface model was $R^2 = 0.997$ (Table S2 and Figure S4). Overall, increasing $E_{p,0}$ and $[\text{PS}]_0$ resulted in higher surfactant

degradation, although the effect of $E_{p,0}$ showed to be less important than that of $[\text{PS}]_0$.

In order to explore the initial persulfate concentration domain, additional experiments were performed by displacing the original design (Figure S3). Previous experiments were maintained (Exps. E1-E7), and three more runs were performed: Exps. E8 ($[\text{PS}]_0 = 12.5 \text{ mmol L}^{-1}$, $E_{p,0} = 0.437 \text{ } \mu\text{mol photons L}^{-1} \text{ s}^{-1}$), E9 ($[\text{PS}]_0 = 15 \text{ mmol L}^{-1}$, $E_{p,0} = 0.324 \text{ } \mu\text{mol photons L}^{-1} \text{ s}^{-1}$), and E10 ($[\text{PS}]_0 = 12.5 \text{ mmol L}^{-1}$, $E_{p,0} = 0.212 \text{ } \mu\text{mol photons L}^{-1} \text{ s}^{-1}$). The fitting by the polynomial model (Eq. 3), considering the complete dataset (Exps. E1-E10, plus the two replicates of Exp. E1) was slightly poorer ($R^2 = 0.979$) than that obtained for the original design, highlighting as significant factors $[\text{PS}]_0$ and $[\text{PS}]_0^2$ (Table S3 and Figure S5). Figure 2 shows the corresponding response surface and contour plot.

$$\begin{aligned} \% \text{Degradation} = & 70.957 + 34.336X_1 + 7.955X_2 \\ & - 12.336X_1^2 + 6.379X_2^2 \\ & - 5.601X_1X_2 \end{aligned} \quad (3)$$

As observed in Figure 2, there is an inflection point regarding optimum $[\text{PS}]_0$ and $E_{p,0}$ values. This point corresponds to about 100% NPEO removal after 120 min of irradiation, as predicted by the model (Eq. 3), for $[\text{PS}]_0 = 10.87 \text{ mmol L}^{-1}$ ($X_1 = 1.195$) and $E_{p,0} = 0.437 \text{ } \mu\text{mol photons L}^{-1} \text{ s}^{-1}$ ($X_2 = 0.866$), respectively; these conditions are between those of Exp. E3 ($[\text{PS}]_0 = 7.75 \text{ mmol L}^{-1}$) and Exp. E8 ($[\text{PS}]_0 = 12.5 \text{ mmol L}^{-1}$), both carried out with $E_{p,0} = 0.437 \text{ } \mu\text{mol photons L}^{-1} \text{ s}^{-1}$. Accordingly, it can be observed by the response surface and contour plot (Figure 2) that there is an improvement in NPEO degradation by raising $[\text{PS}]_0$, which is explained by the higher production of $\text{SO}_4^{\bullet-}$ radicals (Eq. 4) [40].

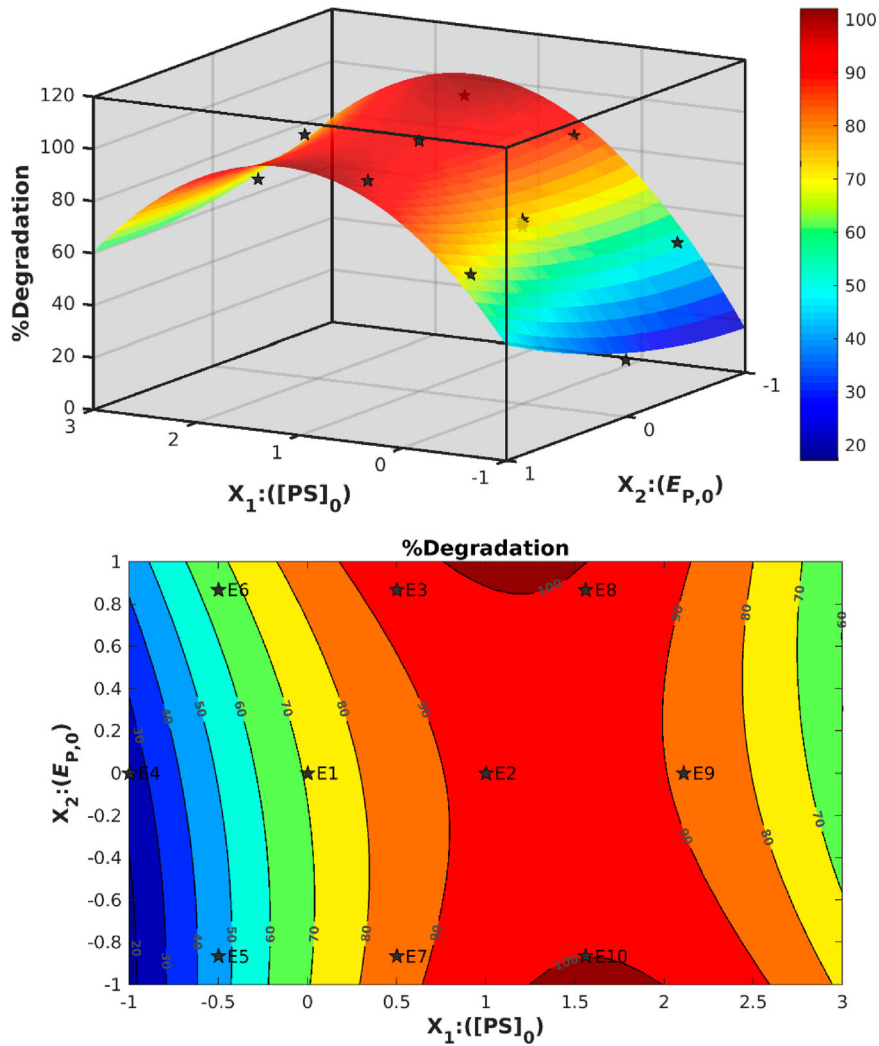
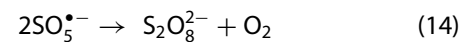
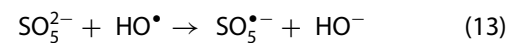
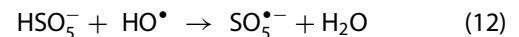
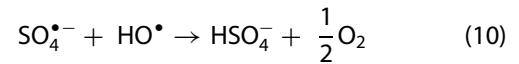
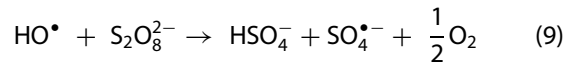
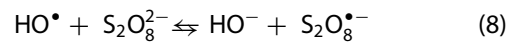
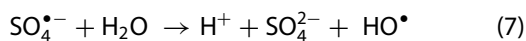
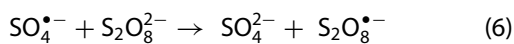
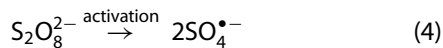
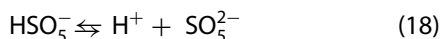
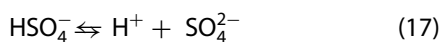
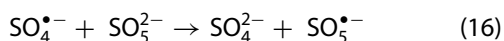


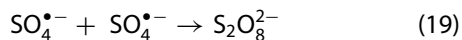
Figure 2. Response surface and contour plot for NPEO % Degradation, varying $[PS]_0$ from 1 to 15 mmol L^{-1} and $E_{p,0}$ from 0.212 to 0.437 $\mu\text{mol photons L}^{-1} \text{s}^{-1}$.

Above a certain concentration, however, NPEO degradation seems to be hampered by the excessive concentration of $S_2O_8^{2-}$ anions, which act as radical scavengers, thereby reducing the availability of reactive free radicals for reacting with contaminant molecules (Eqs. 5–18) [29,41,42]. Similar results were obtained by Arslan-Alaton et al. [26] for the UVC/PS process, who observed total removal of the nonionic surfactant Triton X-45 (octylphenol ethoxylate) for $[PS]_0 \geq 2.5 \text{ mmol L}^{-1}$.





Self-scavenging of $\text{SO}_4^{\bullet-}$ might also occur as reported by Gu et al. [43], who observed the inhibitory effect on ketamine removal caused by the excessive amount of persulfate (Eq. 19):



In our study, it was possible to observe a slight inhibitory effect of persulfate for $[\text{PS}]_0 > 10 \text{ mmol L}^{-1}$ for a greater part of the experimental domain, in agreement with the negative value of the standardised effect of $[\text{PS}]_0^2$ (Figure S5). In fact, for $E_{p,0} = 0.324 \text{ } \mu\text{mol photons L}^{-1} \text{ s}^{-1}$, NPEO removal increased from 21.6% ($[\text{PS}]_0 = 1 \text{ mmol L}^{-1}$) to 69.3% ($[\text{PS}]_0 = 5.5 \text{ mmol L}^{-1}$), and to 96.1% ($[\text{PS}]_0 = 10 \text{ mmol L}^{-1}$), decreasing to 93.1% as $[\text{PS}]_0$ is further increased to 15.0 mmol L^{-1} ; a similar trend was observed for $E_{p,0} = 0.437 \text{ } \mu\text{mol photons L}^{-1} \text{ s}^{-1}$, with removals of 66.7% ($[\text{PS}]_0 = 3.25 \text{ mmol L}^{-1}$), 97.8% ($[\text{PS}]_0 = 7.75 \text{ mmol L}^{-1}$), and 93.2% ($[\text{PS}]_0 = 12.5 \text{ mmol L}^{-1}$). Therefore, it is evident that a higher concentration of the oxidising agent leads to the consumption of reactive radicals by non-activated $\text{S}_2\text{O}_8^{2-}$ anions. Accordingly, Hussain et al. [23] reported that the degradation efficiency of the nonionic surfactant nonylphenol through the nZVI/BC (nanoscale zero-valent iron supported on biochar nanocomposite)-PS system increased from 42.5% to 96.2% by varying $[\text{PS}]_0$ from 1 to 5 mmol L^{-1} , and decreased for $[\text{PS}]_0 > 10 \text{ mmol L}^{-1}$. Nonetheless, our results show that for $E_{p,0} = 0.212 \text{ } \mu\text{mol photons L}^{-1} \text{ s}^{-1}$, the percentage of NPEO removal increased by increasing the persulfate content, from 49.6% ($[\text{PS}]_0 = 3.25 \text{ mmol L}^{-1}$) to 85.9% ($[\text{PS}]_0 = 7.75 \text{ mmol L}^{-1}$), and to 96.0% ($[\text{PS}]_0 = 12.5 \text{ mmol L}^{-1}$), while the response surface predicts the same inhibitory effect of higher initial PS concentrations (i.e. higher than 12.5 mmol L^{-1}). In contrast, the Pareto chart (Figure S5) shows that the standardised effect of $E_{p,0}$ on the ultimate NPEO removal is much lower than that of $[\text{PS}]_0$. Therefore, to observe a significant impact of irradiation, it would be necessary to increase the number of available photons reaching the reaction system by using more lamps, or lamps of higher irradiant power. Nevertheless, our results suggest that increasing $E_{p,0}$ would impact NPEO removal only for $[\text{PS}]_0$ not higher than 8–10 mmol L^{-1} .

The pseudo first-order specific degradation rates (k_{obs}) for NPEO removal through the UVA/PS system, considering the complete dataset (Exps. E1–E10, plus the two

replicates of Exp. E1), varied in the range 0.0020–0.0671 min^{-1} (Table 1), and were positively impacted by all the effects of the independent variables, as confirmed by the ANOVA (F test with p -value < 0.05). The Pareto chart compares the statistically significant values of $[\text{PS}]_0$, $[\text{PS}]_0^2$, $E_{p,0}$, $(E_{p,0})^2$, and the interaction $[\text{PS}]_0 \times E_{p,0}$ (Table S4 and Figure S6). The determination coefficient $R^2 = 0.989$ indicates a good fitting of the experimental data by the response surface model given by Eq. 20:

$$\begin{aligned} k_{\text{obs}}(\text{min}^{-1}) = & 0.00881 + 0.0132X_1 + 0.00605X_2 \\ & + 0.00353X_1^2 + 0.00885X_2^2 \\ & + 0.0105X_1X_2 \end{aligned} \quad (20)$$

Figure 3 suggests a synergistic effect between the oxidant and activation source upon NPEO removal kinetics, with k_{obs} values significantly enhanced when higher $[\text{PS}]_0$ and $E_{p,0}$ were used, although the standardised effect of $[\text{PS}]_0$ showed to be about twice that of $E_{p,0}$; also worth mentioning is the positive value of the interaction $[\text{PS}]_0 \times E_{p,0}$. Furthermore, the positive effect of increasing the amount of oxidant on the surfactant removal rate followed a similar tendency for both $E_{p,0} = 0.212$ and $0.324 \text{ } \mu\text{mol photons L}^{-1} \text{ s}^{-1}$, whereas the k_{obs} values markedly increased with $[\text{PS}]_0$ for $E_{p,0} = 0.437 \text{ } \mu\text{mol photons L}^{-1} \text{ s}^{-1}$.

While the NPEO percent removal achieves a maximum with increasing initial PS concentration, k_{obs} increases linearly with $[\text{PS}]_0$. Accordingly, this tendency depends strongly on $E_{p,0}$, with the impact being almost three-times higher for $E_{p,0} = 0.437 \text{ } \mu\text{mol photons L}^{-1} \text{ s}^{-1}$. Also, whilst a negligible increase in the NPEO removal rate with $E_{p,0}$ was observed for the lowest initial persulfate concentration, the impact of increasing $E_{p,0}$ was particularly significant for $[\text{PS}]_0 = 12.5 \text{ mmol L}^{-1}$, being almost seventeen times higher than that observed for $[\text{PS}]_0 = 3.25 \text{ mmol L}^{-1}$.

These results are in accordance with previous investigations. For example, Méndez-Díaz et al. [25] reported that the k_{obs} for SDBS removal increased linearly with $[\text{K}_2\text{S}_2\text{O}_8]_0$ added to the UVC/ $\text{K}_2\text{S}_2\text{O}_8$ system; by increasing $[\text{K}_2\text{S}_2\text{O}_8]_0$ from $50 \text{ } \mu\text{mol L}^{-1}$ to $300 \text{ } \mu\text{mol L}^{-1}$, the authors verified that k_{obs} increased from $(3.0 \pm 0.5) \times 10^{-3} \text{ s}^{-1}$ to $(1.8 \pm 0.3) \times 10^{-2} \text{ s}^{-1}$. Arslan-Alaton et al. [26] observed a significant improvement in the kinetics of octylphenol ethoxylate (Triton X-45, 20 mg L^{-1}) degradation for $[\text{PS}]_0$ increasing in the range of 0.125 – 1.0 mmol L^{-1} , with degradation rates remaining constant for $[\text{PS}]_0 > 1.0 \text{ mmol L}^{-1}$. For antipyrine degradation through the UVC/PS process, Tan et al. [44] observed that k_{obs} increased from 0.358 h^{-1} to 1.627 h^{-1} with increasing irradiation intensity from 69 to 410 mJ cm^{-2} .

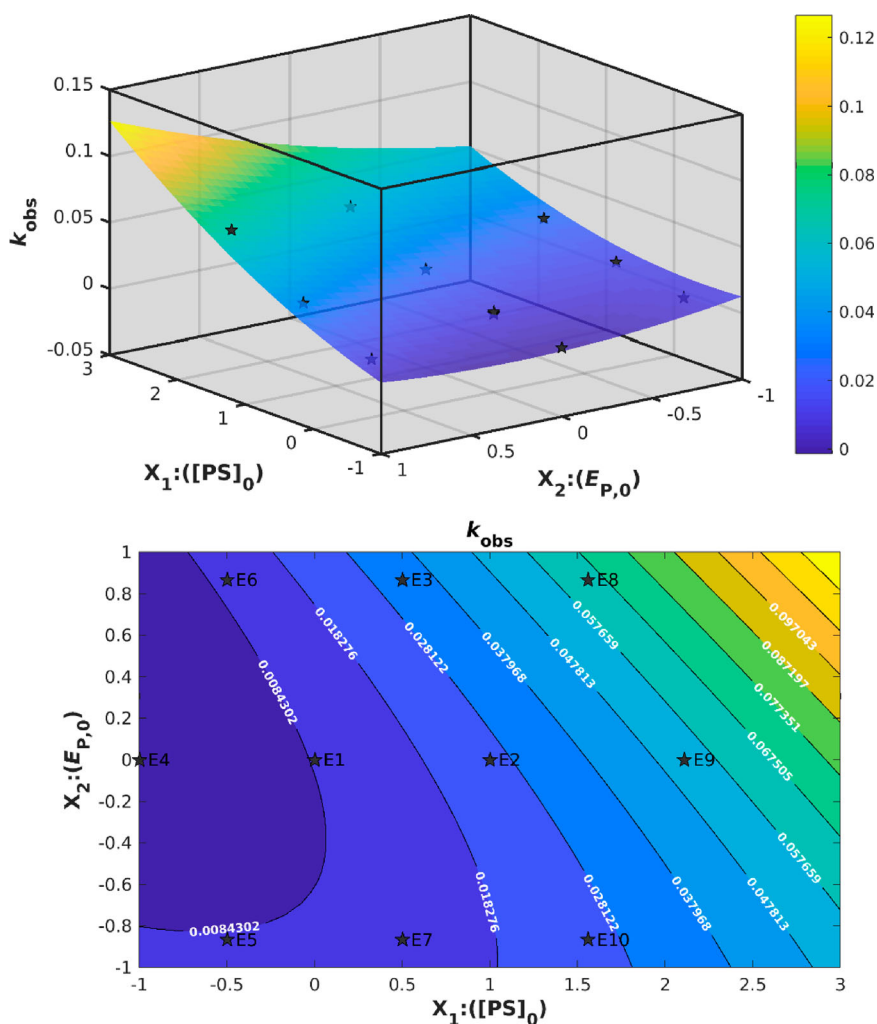


Figure 3. Response surface and contour plot for k_{obs} , varying $[PS]_0$ from 1 to 15 mmol L^{-1} and $E_{P,0}$ from 0.212 to 0.437 $\mu\text{mol photons L}^{-1} \text{s}^{-1}$.

The behaviour of the relative surface tension also proved the efficacy of the process for removing tensoactive substances (Figure 4). By lowering surface tension, surfactants enhance foam formation and stability [45]. Foams hinder the exchange between water and atmospheric air, reducing the concentration of oxygen in water and causing the death by hypoxia of diverse microorganisms [46]. Moreover, Oya et al. [47] evaluated surface tension as an indicator for the acute aquatic toxicity of surfactants. Their results showed that toxic surface tensions of five different surfactants for three aquatic species in 25 mg L^{-1} hardness water varied from 40 to 70 mN m^{-1} . Although surface tension does not represent an absolute factor of toxicity [47], its evaluation must be performed, since lower surface tensions cause an increase in cellular permeability of aquatic species, favouring the entrance of surfactants and other substances in the environment [48].

In our study, lower surface tension reductions relative to Milli-Q® water ($\Delta\gamma_{rel}$) were obtained for higher $[PS]_0$

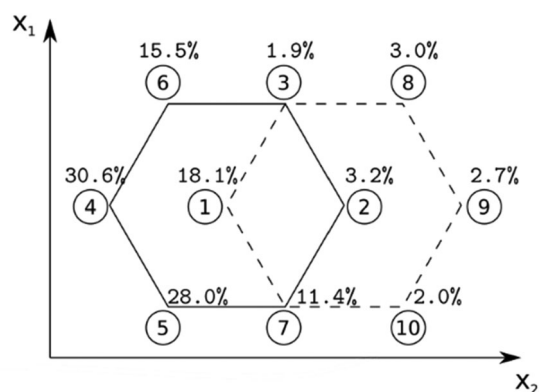


Figure 4. Graphical representation of the Doehlert experimental design according to Table 1, with the values of the surface tension reduction relative to Milli-Q® water (%). Standard error varied from 0.37% to 2.82%.

and $E_{P,0}$, for which high NPEO removals and specific degradation rates were achieved. In that case, the performance of the UVA/PS process can be considered

very effective for the removal of NPEO, forming substances with lower or no tensoactive effect (Figure 4), despite the negligible TOC removals (low mineralisation) observed (results not shown). It is worth observing that the removal of tensoactive activity by the UVA/PS process with increasing initial PS concentration followed similar trends for $E_{P,0} = 0.212$ and $0.324 \mu\text{mol photons L}^{-1} \text{s}^{-1}$, being notably increased for $E_{P,0} = 0.437 \mu\text{mol photons L}^{-1} \text{s}^{-1}$. However, for $[\text{PS}]_0 > 10 \text{ mmol L}^{-1}$, no appreciable differences in $\Delta\gamma_{\text{rel}}$ were observed, with ultimate surface tensions close to that of Milli-Q® water (74.5 mN m^{-1}).

Effect of initial NPEO concentration

It is well known that the initial contaminant concentration may affect the performance of UV/PS processes regarding the removal of different pollutants, as confirmed in previous studies [49,50]. Increasing the initial contaminant concentration reduces the probability of oxidation reactions between pollutants and radicals, therefore decreasing degradation efficiency [51], since the quantities of sulfate and hydroxyl radicals remain constant for higher amounts of pollutant molecules and their intermediates [50]. Herein, the effect of initial NPEO concentration on NPEO degradation was evaluated from $(0.99 \pm 0.13) \text{ mg L}^{-1}$ to $(23.67 \pm 0.85) \text{ mg L}^{-1}$, for fixed $[\text{PS}]_0 = 10 \text{ mmol L}^{-1}$ and $E_{P,0} = 0.324 \mu\text{mol photons L}^{-1} \text{s}^{-1}$.

The results in Figure 5 show that NPEO degradation efficiency decreased by increasing $[\text{NPEO}]_0$. For $[\text{NPEO}]_0 = (0.99 \pm 0.13) \text{ mg L}^{-1}$, k_{obs} was $(0.0700 \pm 0.0026) \text{ min}^{-1}$ ($R^2 = 0.9054$), achieving $(97.2 \pm 0.3) \%$ surfactant removal after 60 min of reaction. For $[\text{NPEO}]_0 = (4.65 \pm 0.15) \text{ mg L}^{-1}$

(Exp. E2 of the Doehlert design), $(96.1 \pm 1.2) \%$ of NPEO was removed, with a specific degradation rate of $(0.0237 \pm 0.0008) \text{ min}^{-1}$ ($R^2 = 0.9566$) after 120 min of reaction. Nevertheless, for $[\text{NPEO}]_0 = (10.12 \pm 0.02) \text{ mg L}^{-1}$, k_{obs} and the percent NPEO removal after 120 min decreased to $(0.0108 \pm 0.0001) \text{ min}^{-1}$ ($R^2 = 0.9941$) and $(74.2 \pm 0.6) \%$, respectively. A further increase in the initial NPEO concentration to $(21.89 \pm 0.09) \text{ mg L}^{-1}$, led to a significant decrease in both k_{obs} and NPEO removal, with ultimate values of $(0.0048 \pm 0.0005) \text{ min}^{-1}$ ($R^2 = 0.9814$) and $(43.3 \pm 3.0) \%$, respectively, after 120 min. A similar effect was observed for the removal of a nonionic surfactant (Triton X-45) by the UVC/ $\text{K}_2\text{S}_2\text{O}_8$ process [23]. The authors obtained almost complete degradation (99–100%) of the target surfactant in less than 40 min of reaction, for initial concentrations ranging from 10 to 100 mg L^{-1} and $[\text{PS}]_0 = 2.5 \text{ mmol L}^{-1}$, even though removal rates were significantly decreased by increasing the initial Triton X-45 concentration.

Considering this issue, we evaluated the effect of reaction time for the highest NPEO concentration used in this study $(23.67 \pm 0.85) \text{ mg L}^{-1}$, over an extended reaction time (Figure 5). The percentage of NPEO removal increased from 43.3% to 73.7% ($k_{\text{obs}} = 0.0055 \pm 0.0001 \text{ min}^{-1}$) ($R^2 = 0.9981$), when increasing the irradiation time from 2 to 4 h. In contrast, our results evidenced that TOC remained practically constant over 4 h of reaction, with less than 1.5% variation. Likewise, Arslan-Alaton et al. [26] observed no TOC removal over 120 min of exposure of a Triton X-45 solution (100 mg L^{-1}) to the UVC/ $\text{K}_2\text{S}_2\text{O}_8$ system. For a higher initial pollutant content, a higher initial concentration of the oxidant agent must thus be applied in combination with the optimisation of the radiation source.

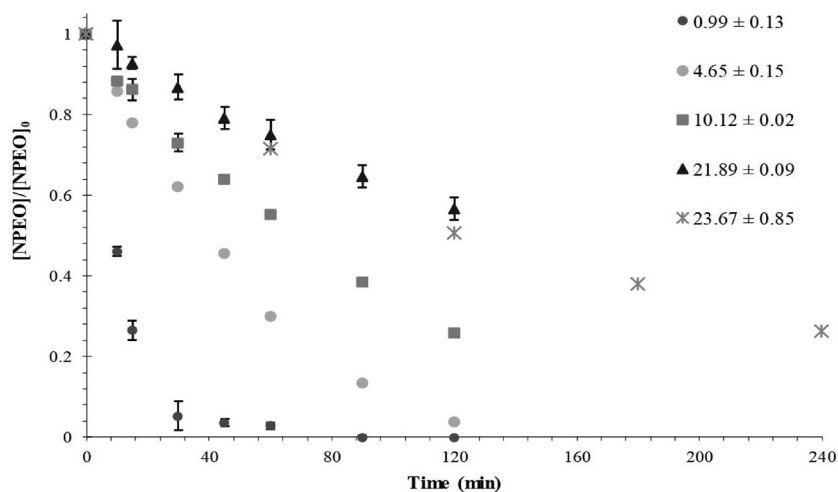


Figure 5. NPEO degradation by the UVA/PS process for different $[\text{NPEO}]_0$ (mg L^{-1}). Conditions: $[\text{PS}]_0 = 10 \text{ mmol L}^{-1}$; $E_{P,0} = 0.324 \mu\text{mol photons L}^{-1} \text{s}^{-1}$.

Finally, the behaviour of surface tension was also evaluated for different NPEO concentrations (Figure 6). Lower surface tension reductions relative to Milli-Q® water were observed for lower $[\text{NPEO}]_0$; nevertheless, as the initial NPEO content increases, lower removals were achieved after 120 min, and the increase in $\Delta\gamma_{\text{rel}}$ is related to the remaining surfactant molecules and/or tensioactive by-products in solution. For the 4 h-experiment, $\Delta\gamma_{\text{rel}}$ diminished from 41.2% to 29.0% (in accordance with the extended NPEO removal), under the same conditions of $[\text{PS}]_0$ and $E_{\text{p},0}$. Therefore, the UVA/PS process shows to be efficient for removing NPEO and tensioactive effect at higher initial concentrations, by exposing the solution to longer irradiation times, even at a lower initial persulfate concentration ($[\text{PS}]_0 = 10 \text{ mmol L}^{-1}$).

Effect of radiation wavelength on NPEO removal

Herein, a comparative study for NPEO removal was accomplished, using UVC (254 nm) for PS activation. Parameters of UVC and UVA lamps used in the experiments are given in Table S5. As remarked in the introduction section, the literature reports values of the molar absorption coefficient of persulfate in the UVC ($13.8\text{--}14 \text{ L mol}^{-1} \text{ cm}^{-1}$, 254 nm) and UVA ($0.25 \text{ L mol}^{-1} \text{ cm}^{-1}$, 351 nm) [17,19]; the quantum yields of sulfate radicals formation at these wavelengths ($\Phi + \text{SO}_4^{\bullet-}$) are 1.4 and 0.5 mol $\text{SO}_4^{\bullet-} \text{ mol photons}^{-1}$, respectively [19]. NPEO degradation for different initial concentrations and number of lamps is summarised in Figure 7.

NPEO degradation by the UVC/PS process resulted in higher k_{obs} and percent removals, when compared with the UVA/PS process for the lowest $[\text{PS}]_0$ of the Doehlert

design (1 mmol L^{-1}). For $[\text{NPEO}]_0 = (5.0 \pm 0.2) \text{ mg L}^{-1}$, and $E_{\text{p},0} = 0.338 \mu\text{mol photons L}^{-1} \text{ s}^{-1}$, 96.9% of NPEO was removed, with $k_{\text{obs}} = 0.0369 \text{ min}^{-1}$. This behaviour is expected, given the higher value of ϵ_{254} and Φ ($+\text{SO}_4^{\bullet-}$), therefore resulting in enhanced persulfate anions activation and formation of $\text{SO}_4^{\bullet-}$ for NPEO removal. However, for the highest initial NPEO concentration, $[\text{NPEO}]_0 = (17.0 \pm 0.1) \text{ mg L}^{-1}$, when $E_{\text{p},0}$ was reduced from 0.338 to $0.141 \mu\text{mol photons L}^{-1} \text{ s}^{-1}$, NPEO percent removal decreased from $(73.4 \pm 6.2) \%$ to $(49.6 \pm 2.0) \%$ and k_{obs} decreased from $(0.011 \pm 0.002) \text{ min}^{-1}$ to $(0.0059 \pm 0.0004) \text{ min}^{-1}$, respectively. A similar behaviour was reported in previous studies for the degradation of different compounds, in which high pollutant concentrations resulted in lower removal efficiencies: Triton X-45, by means of the UVC/PS process [26]; 2,4,6-trichlorophenol, through peroxymonosulfate/activated carbon/UVC [50]; amicarbazono, by UVA/persulfate [31]; and the artificial sweetener sucralose, using UVC/ peroxymonosulfate [51].

The UVC/PS process has been mostly applied to the degradation of nonionic and anionic surfactants [25–28]. Nevertheless, note that for a low initial surfactant concentration, both UVC/PS and UVA/PS processes showed similar performances in terms of removal rate and ultimate percent removal, when higher $[\text{PS}]_0$ was used for the latter. In fact, in Exp. E2 of the Doehlert design (UVA/PS, $[\text{NPEO}]_0 = (4.65 \pm 0.15) \text{ mg L}^{-1}$, $[\text{PS}]_0 = 10 \text{ mmol L}^{-1}$, and $E_{\text{p},0} = 0.324 \mu\text{mol photons L}^{-1} \text{ s}^{-1}$), 96.1% NPEO removal was achieved with a specific degradation rate of 0.0237 min^{-1} , while for the UVC/PS system, for an initial persulfate concentration ten times lower (1 mmol L^{-1}) and $E_{\text{p},0} = 0.338 \mu\text{mol photons L}^{-1} \text{ s}^{-1}$, 96.9% NPEO was removed with k_{obs} was 0.0369 min^{-1} .

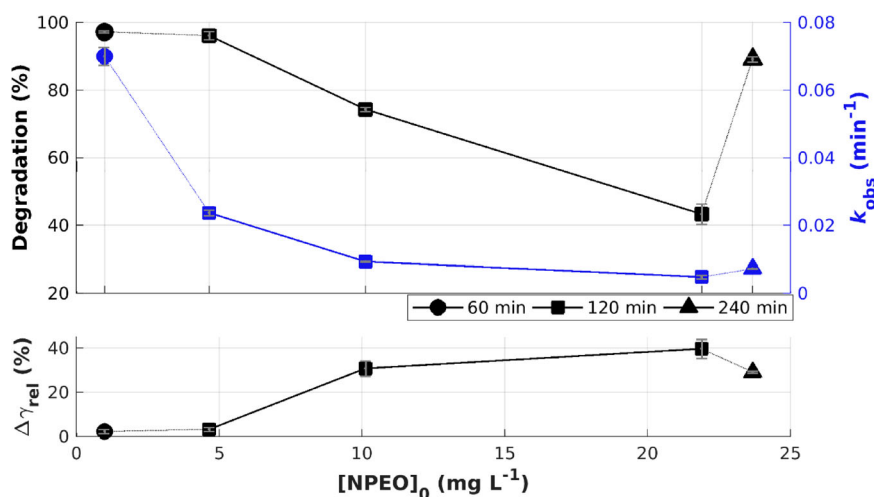


Figure 6. NPEO % Degradation, k_{obs} , and surface tension reductions relative to Milli-Q® water for the UVA/PS process, varying $[\text{NPEO}]_0$. Conditions: $[\text{PS}]_0 = 10 \text{ mmol L}^{-1}$, $E_{\text{p},0} = 0.324 \mu\text{mol photons L}^{-1} \text{ s}^{-1}$.

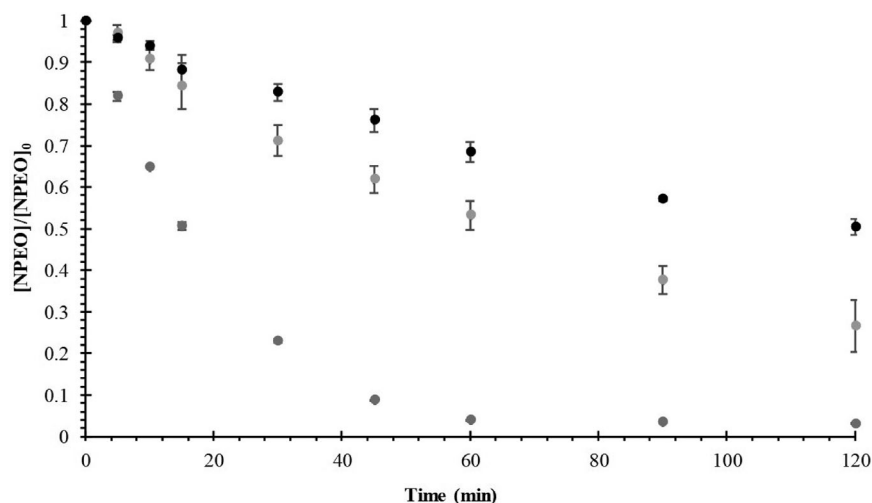


Figure 7. NPEO degradation by the UVC/PS process for different conditions of $E_{p,0}$ ($\mu\text{mol photons L}^{-1} \text{s}^{-1}$)/ $[\text{NPEO}]_0$ (mg L^{-1}) and $[\text{PS}]_0 = 1 \text{ mmol L}^{-1}$. • $0.338/5.0 \pm 0.2$. • $0.338/17.0 \pm 0.1$. • $0.141/17.0 \pm 0.1$.

This result is important because it highlights that the UVA/PS process can be advantageously used for NPEO removal at lower initial concentrations when compared to UVC/PS, particularly if the UVA radiation of the sunlight spectrum, which is about 4.5% of the solar irradiance reaching the Earth's surface [52] is used, since the costs of irradiated persulfate-based processes are mainly related to energy consumption.

As observed for the UVA/PS system, lower surface tension reductions relative to Milli-Q® water were obtained for the UVC/PS process, when higher NPEO percent removals and k_{obs} were achieved (Figure 8). The lowest $\Delta\gamma_{\text{rel}}$ (3.1%) through the UVC/PS process was obtained for $[\text{NPEO}]_0 = (5.0 \pm 0.2) \text{ mg L}^{-1}$, $[\text{PS}]_0 = 1 \text{ mmol L}^{-1}$, and $E_{p,0} = 0.338 \mu\text{mol photons L}^{-1} \text{s}^{-1}$. This result is comparable to that obtained for Exp. E2 ($\Delta\gamma_{\text{rel}} = 3.2\%$).

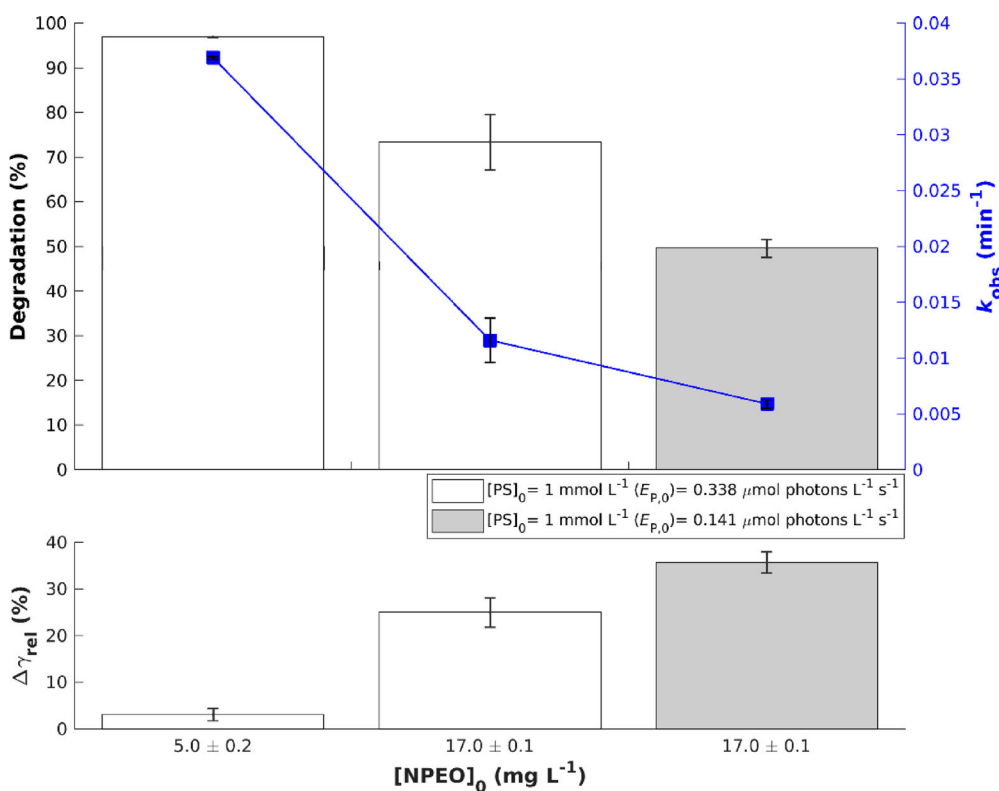
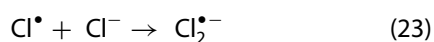


Figure 8. NPEO % Degradation, k_{obs} , and surface tension reductions relative to Milli-Q® water for the UVC/PS process, varying $[\text{NPEO}]_0$.

Effect of real wastewater on NPEO removal through the UVA/PS process

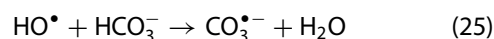
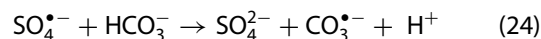
Dissolved organic matter and some anions such as Cl^- , NO_3^- , NO_2^- are found in most real water matrices and act as radical scavengers with adverse effects on UV-based processes [51]. It is worth mentioning that surfactants degradation by means of UV/PS processes have been exclusively investigated in aqueous model systems. In the present work, the performance of UVA/PS for removing NPEO from a real water matrix sampled from a WWTP was studied. After decanted and characterised, this sample was spiked with $(1.43 \pm 0.03) \text{ mg L}^{-1}$ of NPEO, and the experiment was conducted with $[\text{PS}]_0 = 10 \text{ mmol L}^{-1}$ and $E_{P,0} = 0.324 \mu\text{mol photons L}^{-1} \text{ s}^{-1}$.

The results in Figure S7 show that NPEO degradation was significantly hindered in the real water matrix used, in comparison with that observed in Milli-Q® water, which can be attributed to the presence of Cl^- anions at concentrations up to 45.5 mg L^{-1} in the wastewater sample, due to the transformation of $\text{SO}_4^{\bullet-}$ and HO^\bullet radicals into less reactive Cl^\bullet and $\text{Cl}_2^{\bullet-}$ species (Eqs. 21–23) [53,54]. Cl^- at concentrations of $35.5\text{--}142 \text{ mg L}^{-1}$ was also found to inhibit the removal of artificial sweeteners by UVC/PS [54], and of ketoprofen through heat-activated persulfate in seawater matrix [53].



Moreover, the presence of co-solutes such as HCO_3^- (alkalinity of about 300 mg L^{-1}) and organic/inorganic matter in the wastewater sample ($\text{TOC} = 10.5 \text{ mg L}^{-1}$; $\text{COD} = 80 \text{ mg O}_2 \text{ L}^{-1}$) can scavenge $\text{SO}_4^{\bullet-}$ and HO^\bullet radicals, decreasing NPEO degradation efficiency. In fact, bicarbonate anions react with $\text{SO}_4^{\bullet-}$ and HO^\bullet (Eqs. 24–25) with rate constants of $2.8 \times 10^6 \text{ L mol}^{-1} \text{ s}^{-1}$ and $8.5 \times 10^6 \text{ L mol}^{-1} \text{ s}^{-1}$, respectively, therefore reducing contaminants degradation efficiency [55]. The same behaviour was observed in previous studies regarding the removal of other pollutants through UV/PS [54,56,57]. Notwithstanding, some studies reported opposite effects, with faster pollutant degradation observed in the presence of bicarbonate anions, which was attributed to the catalytic effect of carbonate species in activated-persulfate systems [58]. Finally, the inner-filter effect of the real matrix diminishes the solution transparency, decreasing the amount of UV photons available for PS activation, as reported by Sharma et al. [56] for bisphenol degradation through

the UVC/peroxymonosulfate process.



Acute toxicity tests

The literature reports the production of shorter-ethoxy chain compounds with higher toxicity in oxidative treatments of APEOs (alkylphenol ethoxylates) [59]. Considering this issue, toxicity tests were performed before and after the UVA/PS treatment for the condition of higher NPEO removal achieved by the Doehlert experimental design (Exp. E3: $[\text{PS}]_0 = 7.75 \text{ mmol L}^{-1}$; $E_{P,0} = 0.437 \mu\text{mol photons L}^{-1} \text{ s}^{-1}$; $[\text{NPEO}]_0 = 4.65 \pm 0.15 \text{ mg L}^{-1}$), using the microcrustacean *D. similis*. The results revealed that the toxicity did not differ significantly for untreated and treated solutions, with values of $\text{EC}_{50-48 \text{ h}} (\% \text{ v/v})$ equal to $(17.7 \pm 2.5) \%$ and $(18.9 \pm 1.8) \%$, respectively, suggesting that no more toxic by-products against *D. similis* were formed under the experimental conditions evaluated in the present study, which does not necessarily mean the absence of toxicity against aquatic microorganisms. Therefore, further evaluation under different treatment conditions and with different test organisms must be performed to better characterise the residual toxicity of NPEO solutions treated by UVA/PS.

Conclusions

The UVA/ $\text{S}_2\text{O}_8^{2-}$ (UVA/PS) process showed to be efficient for nonylphenol polyethoxylate (NPEO) removal ($[\text{NPEO}]_0$ of about 5 mg L^{-1}), by using $[\text{PS}]_0 > 5.5 \text{ mmol L}^{-1}$, with percent removals higher than 70%, and specific degradation rates higher than 0.0093 min^{-1} . The highest values achieved were 97.8% degradation ($[\text{PS}]_0 = 7.75 \text{ mmol L}^{-1}$) and pseudo first-order specific degradation rate (k_{obs}) of 0.0320 min^{-1} , for $E_{P,0} = 0.437 \mu\text{mol photons L}^{-1} \text{ s}^{-1}$. This result is important because it reveals good efficiency of UVA/PS for removing NPEO at concentrations equivalent to those found in different water matrices. In addition, the acute toxicities of untreated and treated solutions towards *Daphnia similis* were similar, suggesting that no by-products more toxic than the parent compound, against this specific microorganism, were generated following NPEO degradation under the experimental conditions evaluated in the present study. Moreover, the simultaneous effect of $[\text{PS}]_0$ and $E_{P,0}$ on NPEO removal by UVA/PS had not been explored in literature. With this aim, our results showed that higher values of $E_{P,0}$ would influence NPEO removal for initial persulfate concentrations not higher than $8\text{--}10 \text{ mmol L}^{-1}$.

Nevertheless, the presence of high concentrations of inhibitory constituents in real wastewater, along with turbidity impacted NPEO removal, suggesting the need of optimising treatment conditions for each specific application, besides an efficient pre-treatment.

Higher initial NPEO concentrations negatively affected UVA/PS performance, with no significant TOC removals (less than 1.5%) due to the insufficient amount of persulfate. Nevertheless, it should be remarked that the TOC levels corresponding to the range of initial NPEO concentrations selected ($\sim 1\text{--}24\text{ mg L}^{-1}$) and usually reported in the literature for real water matrices, were remarkably low, not posing a risk to the aquatic environment. Furthermore, the application of a longer reaction time (4 h) for the highest $[\text{NPEO}]_0$ ($\sim 22\text{--}24\text{ mg L}^{-1}$) resulted in more than 70% NPEO degradation, $k_{\text{obs}} = 0.0055\text{ min}^{-1}$, and ΔY_{rel} of 29%. In terms of radiation wavelength, for lower $[\text{NPEO}]_0$, both UVC and UVA-driven persulfate based processes showed similar performances, when the latter operated under optimal conditions ($[\text{PS}]_0 = 10\text{ mmol L}^{-1}$; $E_{\text{p},0} = 0.324\text{ }\mu\text{mol photons L}^{-1}\text{ s}^{-1}$), with NPEO degradation higher than 96% and similar tensoactivity removals. Therefore, the UVA/PS process could advantageously use the UVA radiation available in solar light for NPEO removal at concentrations usually found in wastewater.

Additionally, the surface tension measurements of treated solutions confirmed the efficacy of the UVA/PS process for tensoactivity removal, despite the negligible mineralisation (i.e. low TOC removal) achieved, suggesting that NPEO degradation by-products do not exhibit tensoactive character. Lower surface tension reductions relative to Milli-Q® water (ΔY_{rel}), within the range 2%–3%, were obtained for higher $[\text{PS}]_0$ and $E_{\text{p},0}$, for which high NPEO removals and specific degradation rates were achieved. Surface tension measurements can therefore be a simple, useful diagnosis for evaluating the treatment process efficacy.

Acknowledgments

This study has been supported by Conselho Nacional de Desenvolvimento Científico e Tecnológico (CNPq, Brazil).

Disclosure statement

No potential conflict of interest was reported by the authors.

Funding

This work was supported by Conselho Nacional de Desenvolvimento Científico e Tecnológico (CNPq, Brazil) [grant number 140657/2018-5].

ORCID

R. F. Nunes  <http://orcid.org/0000-0003-1758-5351>

F. K. Tominaga  <http://orcid.org/0000-0002-4733-8370>

S. I. Borrely  <http://orcid.org/0000-0002-9692-5539>

A. C. S. C. Teixeira  <http://orcid.org/0000-0002-2790-2704>

References

- [1] Patel N, Khan MD, Shahane S. et al. Emerging pollutants in aquatic environment: source, effect, and challenges in biomonitoring and bioremediation - a review. *Pollution*. 2020;6(1). doi:10.22059/poll.2019.285116.646
- [2] Arslan A, Topkaya E, Bingöl D, et al. Removal of anionic surfactant sodium dodecyl sulfate from aqueous solutions by $\text{O}_3/\text{UV}/\text{H}_2\text{O}_2$ advanced oxidation process: process optimization with response surface methodology approach. *Sustainable Environ Res*. 2018;28:65–71. doi:10.1016/j.serj.2017.11.002
- [3] Aun HW, Hu HW, Wang L, et al. The bioconcentration and degradation of nonylphenol and nonylphenol polyethoxylates by *Chlorella vulgaris*. *Int J Mol Sci*. 2014;15:1255–1270. doi:10.3390/ijms15011255
- [4] Shiu R-F, Jiang J-J, Kao H-Y, et al. Alkylphenol ethoxylate metabolites in coastal sediments off southwestern Taiwan: spatiotemporal variations, possible sources, and ecological risk. *Chemosphere*. 2019;225:9–18. doi:10.1016/j.chemosphere.2019.02.136
- [5] González S, Petrovic M, Radetic M, et al. Characterization and quantitative analysis of surfactants in textile wastewater by liquid chromatography/quadrupole-time-of-flight mass spectrometry. *Rapid Commun Mass Spectrom*. 2008;22:1445–1454. doi:10.1002/rcm.3527.
- [6] Ying GG. Fate, behavior and effects of surfactants and their degradation products in the environment. *Environ Int*. 2006;32:417–431. doi:10.1016/j.envint.2005.07.004
- [7] Lee HB, Peart TE, Gris G, et al. Endocrine-disrupting chemicals in industrial wastewater samples in Toronto, Ontario. *Water Qual Res J*. 2002;37(2):459–472. doi:10.2166/wqrj.2002.030
- [8] Henriques DM K, Mayer K, et al. FM. Nonylphenol polyethoxylate in hospital wastewater: a study of the subproducts of electrocoagulation. *J Environ Sci Health, A*. 2012;47(3):497–505. doi:10.1080/10934529.2012.640249
- [9] Jardak K, Drogui P, Daghbir R. Surfactants in aquatic and terrestrial environment: occurrence, behavior, and treatment processes. *Environ Sci Pollut Res*. 2016;23:3195–3216. doi:10.1007/s11356-015-5803-x
- [10] Patil VV, Gogate PR, Bhat AP, et al. Treatment of laundry wastewater containing residual surfactants using combined approaches based on ozone, catalyst and cavitation. *Sep Purif Technol*. 2020;239:1–9. doi:10.1016/j.seppur.2020.116594
- [11] Wang L, Xiao H, He N, et al. Biosorption and biodegradation of the environmental hormone nonylphenol by four marine microalgae. *Sci Rep*. 2019;9(1):1–11. doi:10.1038/s41598-019-41808-8
- [12] Spehar RL, Brooke LT, Markee TP, et al. Comparative toxicity and bioconcentration of nonylphenol in freshwater organisms. *Environ Toxicol Chem*. 2010;29(9):2104–2111. doi:10.1002/etc.262

- [13] Gao QT, Tam NFY. Growth, photosynthesis and antioxidant responses of two microalgal species, *Chlorella vulgaris* and *Selenastrum capricornutum*, to nonylphenol stress. *Chemosphere*. 2011;82(3):346–354. doi:10.1016/j.chemosphere.2010.10.010
- [14] Hamlin HJ, Marciano K, Downs CA. Migration of nonylphenol from food-grade plastic is toxic to the coral reef fish species *Pseudochromis fridmani*. *Chemosphere*. 2015;139:223–228. doi:10.1016/j.chemosphere.2015.06.032
- [15] Kim A-RU, Kim S-H, Kim D, et al. Detection of nonylphenol with a gold-nanoparticle-based small-molecule sensing system using an ssDNA aptamer. *Int J Mol Sci*. 2020;21(208):1–11. doi:10.3390/ijms21010208
- [16] Silveira JE, Cardoso TO, Rodrigues MB, et al. Electro activation of persulfate using iron sheet as low-cost electrode: the role of the operating conditions. *Environ Technol*. 2018;39(9):1208–1216. doi:10.1080/09593330.2017.1323960
- [17] Stefan MI. Advanced oxidation processes for water treatment: fundamentals and applications. London: IWA publishing; 2018, p. 430–431.
- [18] Ershov BG, Gordeev AV, Seliverstov AF. Ozone solubility in aqueous solutions of NaCl, Na₂SO₄, and K₂SO₄: application of the Weisenberger-Schumpe model for description of regularities and calculation of the ozone molar absorption coefficient. *Ozone: Sci Eng*. 2017;39(2):69–79. doi:10.1080/01919512.2016.1262239
- [19] Herrmann H. On the photolysis of simple anions and neutral molecules as sources of O[•]/OH, SO₃[•] and Cl in aqueous solution. *Phys Chem Chem Phys*. 2007;9:3935–3964. doi:10.1039/B618565G
- [20] Cataldo F. Hydrogen peroxide photolysis with different UV light sources including a new UV-LED light source. *New Front Chem*. 2014;23:99–110.
- [21] Hart EJ. Molar absorptivities of ultraviolet and visible bands of ozone in aqueous solutions. *Anal Chem*. 1983;55(1):46–49. doi:10.1021/ac00252a015
- [22] Ioannidi A, Frontistis Z, Mantzavinos D. Destruction of propyl paraben by persulfate activated with UV-A light emitting diodes. *J Environ Chem Eng*. 2018;6:2992–2997. doi:10.1016/j.jece.2018.04.049
- [23] Hussain I L, Zhang M, et al Y. Insights into the mechanism of persulfate activation with nZVI/BC nanocomposite for the degradation of nonylphenol. *Chem Eng J*. 2017;311:163–172. doi:10.1016/j.cej.2016.11.085
- [24] Samarghandi MR, Mehralipour J, Azarian G, et al. Decomposition of sodium dodecylbenzene sulfonate surfactant by electro/Fe²⁺-activated persulfate process from aqueous solutions. *Global NEST J*. 2019;19(1):115–121. doi:10.30955/gnj.002063
- [25] Méndez-Díaz J, Sánchez-Polo M, Rivera-Utrilla J, et al. Advanced oxidation of the surfactant SDBS by means of hydroxyl and sulphate radicals. *Chem Eng J*. 2010;163:300–306. doi:10.1016/j.cej.2010.08.002
- [26] Arslan-Alaton I, Olmez-Hanci T, Genç B, et al. Advanced oxidation of the commercial nonionic surfactant octylphenol polyethoxylate TritonTM X-45 by the persulfate/UV-C process: effect of operating parameters and kinetic evaluation. *Front Chem*. 2013;1:1–7. doi:10.3389/fchem.2013.00004
- [27] Olmez-Hanci T, Arslan-Alaton I, Genc B. Degradation of the nonionic surfactant TritonTM X-45 with HO[•] and SO₄^{•-}-based advanced oxidation processes. *Chem Eng J*. 2014;239:332–340. doi:10.1016/j.cej.2013.11.033
- [28] Kabdasli I, Ecer Ç, Olmez-Hanci T, et al. A comparative study of HO[•]- and SO₄^{•-}-based AOPs for the degradation of non-ionic surfactant Brij30. *Water Sci Technol*. 2015;72:194–202. doi:10.2166/wst.2015.204
- [29] Wang J, Wang S. Activation of persulfate (PS) and peroxymonosulfate (PMS) and application for the degradation of emerging contaminants. *Chem Eng J*. 2018;334:1502–1517. doi:10.1016/j.cej.2017.11.059
- [30] Palharim PH, Graça, CAL, Teixeira, ACSC. Comparison between UVA-and zero-valent iron-activated persulfate processes for degrading propylparaben. *Environ Sci Pollut Res*. 2020;27:22214–22224. doi:10.1007/s11356-020-08141-4
- [31] Graça CAL, Velosa AC, Teixeira ACSC. Amicarbazone degradation by UVA-activated persulfate in the presence of hydrogen peroxide or Fe²⁺. *Catal Today*. 2017;280:80–85. doi:10.1016/j.cattod.2016.06.044
- [32] Jurado E, Fernández-Serrano M, Núñez-Olea J, et al. Aerobic biodegradation of a nonylphenol polyethoxylate and toxicity of the biodegradation metabolites. *Bull Environ Contam Toxicol*. 2009;83(3):307–312. doi:10.1007/s00128-009-9716-6
- [33] Doehlert DH. Uniform shell designs. *J R Stat Soc Ser C Appl Stat*. 1970;19:231–239. doi:10.2307/2346327
- [34] Ferreira SLC Q, Fernandes AS, et al MS. Application of factorial designs and Doehlert matrix in optimization of experimental variables associated with the preconcentration and determination of cadmium and copper in seawater by inductively coupled plasma optical emission spectrometry. *Spectrochim Acta Part B*. 2002;57:1939–1950. doi:10.1016/S0584-8547(02)00160-X
- [35] Novaes CG, Yamaki RT, De Paula F, et al. Otimização de métodos analíticos usando metodologia de superfícies de resposta - parte I: Variáveis de processo. *Revista Virtual de Química*. 2017;9(3):1184–1215. doi:10.21577/1984-6835.20170070
- [36] ABNT. ABNT NBR 12713 Aquatic ecotoxicology – Acute toxicity – Test with *Daphnia spp* (Crustacea, Cladocera). 2016.
- [37] Hamilton MA, Russo RC, Thurston RV. Trimmed Spearman-Kärber method for estimating median lethal concentrations in toxicity bioassays. *Environ Sci Technol*. 1977;11:714–719. doi:10.1021/es60130a004
- [38] Iqbal M, Bhatti IA. Gamma radiation/H₂O₂ treatment of a nonylphenol ethoxylates: degradation, cytotoxicity, and mutagenicity evaluation. *J Hazard Mater*. 2015;299:351–360. doi:10.1016/j.jhazmat.2015.06.045
- [39] Chen L, Zhou H-Y, Deng Q-Y. Photolysis of nonylphenol ethoxylates: the determination of the degradation kinetics and the intermediate products. *Chemosphere*. 2007;68:354–359. doi:10.1016/j.chemosphere.2006.12.055
- [40] Ucuñ OK, Montazeri B, Arslan-Alaton I, et al. Degradation of 3,5-dichlorophenol by UV-C photolysis and UV-C-activated persulfate oxidation process in pure water and simulated tertiary treated urban wastewater. *Environ Technol*. 2020. doi:10.1080/09593330.2020.1732478
- [41] Kattel E, Kaur B, Trapido M, et al. Persulfate-based photodegradation of a beta-lactam antibiotic amoxicillin in various water matrices. *Environ Technol*. 2020;41(2): 202–210. doi:10.1080/09593330.2018.1493149

- [42] Yang Y, Ji Y, Yang P, et al. UV-activated persulfate oxidation of the insensitive munitions compound 2,4-dinitroanisole in water: kinetics, products, and influence of natural photoinducers. *J Photochem Photobiol A*. 2018;360:188–195. doi:10.1016/j.jphotochem.2018.04.044
- [43] Gu D, Guo C, Hou S, et al. Kinetic and mechanistic investigation on the decomposition of ketamine by UV-254 nm activated persulfate. *Chem Eng J*. 2019;370:19–26. doi:10.1016/j.cej.2019.03.093
- [44] Tan C, Gao N, Deng Y, et al. Degradation of antipyrine by UV, UV/H₂O₂ and UV/PS. *J Hazard Mater*. 2013;260:1008–1016. doi:10.1016/j.jhazmat.2013.06.060
- [45] Feneuil B, Pitois O, Roussel N. Effect of surfactants on the yield stress of cement paste. *Cem Concr Res*. 2017;100:32–39. doi:10.1016/j.cemconres.2017.04.015
- [46] Yuan CL, Xu ZZ, Fan MX, et al. Study on characteristics and harm of surfactants. *J Chem Pharm Res*. 2014;6(7):2233–2237.
- [47] Oya M, Orito S, Ishikawa Y, et al. Effects of water hardness and existence of adsorbent on toxic surface tension of surfactants for aquatic species. *J Oleo Sci*. 2007;56(5):237–243. doi:10.5650/jos.56.237
- [48] Hisano N, Oya M. Effects of surface activity on aquatic toxicity of binary surfactant mixtures. *J Oleo Sci*. 2010;59(11):589–599. doi:10.5650/jos.59.589
- [49] Bu L, Zhou S, Shi Z, et al. Degradation of oxcarbazepine by UV-activated persulfate oxidation: kinetics, mechanisms, and pathways. *Environ Sci Pollut Res*. 2016;23:2848–2855. doi:10.1007/s11356-015-5524-1
- [50] Ghanbari F, Moradi M, Gohari F. Degradation of 2,4,6-trichlorophenol in aqueous solutions using peroxymonosulfate/activated carbon/UV process via sulfate and hydroxyl radicals. *J Water Process Eng*. 2016;9:22–28. doi:10.1016/j.jwpe.2015.11.011
- [51] Xu Y, Lin Z, Wang Y, et al. The UV/peroxymonosulfate process for the mineralization of artificial sweetener sucralose. *Chem Eng J*. 2017;317:561–569. doi:10.1016/j.cej.2017.02.058
- [52] Oppenländer T. Photochemical purification of water and air: advanced oxidation processes (AOPs): principles, reaction mechanisms, reactor concepts. Wiley-VCH, 2003. doi:10.1002/9783527610884
- [53] Feng Y, Song Q, Lv W, et al. Degradation of ketoprofen by sulfate radical-based advanced oxidation processes: kinetics, mechanisms, and effects of natural water matrices. *Chemosphere*. 2017;189:643–651. doi:10.1016/j.chemosphere.2017.09.109
- [54] Fu Y, Wu G, Geng J, et al. Kinetics and modeling of artificial sweeteners degradation in wastewater by the UV/persulfate process. *Water Res*. 2019;150:12–20. doi:10.1016/j.watres.2018.11.051
- [55] Ghauch A, Tuqan AM. Oxidation of bisoprolol in heated persulfate/H₂O systems: kinetics and products. *Chem Eng J*. 2012;183:162–171. doi:10.1016/j.cej.2011.12.048
- [56] Sharma J, Mishra IM, Dionysiou DD, et al. Oxidative removal of bisphenol a by UV-C/peroxymonosulfate (PMS): kinetics, influence of co-existing chemicals and degradation pathway. *Chem Eng J*. 2015;276:193–204. doi:10.1016/j.cej.2015.04.021
- [57] Xie P, Ma J, Liu W, et al. Removal of 2-MIB and geosmin using UV/persulfate: contributions of hydroxyl and sulfate radicals. *Water Res*. 2015;69:223–233. doi:10.1016/j.watres.2014.11.029
- [58] Graça CAL, Fujita LTN, Velosa AC, et al. Amicarbazone degradation promoted by ZVI-activated persulfate: study of relevant variables for practical application. *Environ Sci Pollut Res*. 2018;25:5474–5483. doi:10.1007/s11356-017-0862-9
- [59] Omez-Hanci T, Arslan-Alaton I, Dursun D, et al. Degradation and toxicity assessment of the nonionic surfactant Triton™ X-45 by the peroxymonosulfate/UV-C process. *Photochem Photobiol Sci*. 2015;14:569–575. doi:10.1039/c4pp00230j